

# Consideration of Photon Radiation in Kinematic Fits for Future $e^+e^-$ Colliders

Moritz Beckmann<sup>1,2</sup>, Benno List<sup>2</sup> and Jenny List<sup>1</sup>

1 - DESY, Notkestr. 85, 22607 Hamburg, Germany

2 - University of Hamburg, Institute for Experimental Physics  
Luruper Chaussee 149, 22761 Hamburg, Germany

Kinematic fitting is an important tool to improve the resolution in high-energy physics experiments. At future  $e^+e^-$  colliders, photon radiation parallel to the beam carrying away large amounts of energy and momentum will become a challenge for kinematic fitting. A photon with longitudinal momentum  $p_{z,\gamma}(\eta)$  is introduced, which is parametrized such that  $\eta$  follows a normal distribution. In the fit,  $\eta$  is treated as having a measured value of zero, which corresponds to  $p_{z,\gamma} = 0$ . As a result, fits with constraints on energy and momentum conservation converge well even in the presence of a highly energetic photon, while the resolution of fits without such a photon is retained. A fully simulated and reconstructed  $e^+e^- \rightarrow q\bar{q}q\bar{q}$  event sample at  $\sqrt{s} = 500$  GeV is used to investigate the performance of this method under realistic conditions, as expected at the International Linear Collider.

## 1 Introduction

Radiation of photons at angles so small that they escape along the beam pipe is usually not taken into account in kinematic fits. At previous  $e^+e^-$  colliders such as LEP, the losses due to photon radiation were acceptable [1]. At future facilities such as the International Linear Collider (ILC) or the Compact Linear Collider (CLIC), photon radiation will be much stronger due to higher center-of-mass energies and stronger focussing of the beams.

This paper presents a novel method to take the energy and longitudinal momentum of photon radiation into account in kinematic fits. A priori information about the momentum spectrum of photon radiation is used to treat the photon's momentum as a measured parameter in the fit. As a test case, the production of  $W^+W^-/Z^0Z^0$  pairs decaying to light quark jets at the ILC is considered, with fully simulated Monte Carlo events as reconstructed by the International Large Detector (ILD) [2]. A more detailed description of the underlying concept can be found in [3] and a more detailed description of the method and its application tests in [4].

## 2 Representation of the photon

The simplest method to cope with highly energetic photons escaping the detector along the beam pipe in a constrained kinematic fit is therefore to drop the energy and longitudinal momentum conservation constraints, thus losing two degrees of freedom.

Here the photon is treated as a particle with a measured momentum of zero and an uncertainty derived from its known momentum spectrum. For this purpose, the photon momentum  $p_{z,\gamma}$  is transformed into a quantity  $\eta$  which follows a Gaussian distribution [3]:

$$p_{z,\gamma}(\eta) = \text{sign}(\eta) E_{\text{max}} \left[ \text{erf}(|\eta|/\sqrt{2}) \right]^{\frac{1}{\beta}} \quad (1)$$

$E_{\text{max}}$  is the maximum possible energy for a single ISR photon. The exponent  $\beta$  is given by

$$\beta = \frac{2\alpha}{\pi} \left( \ln \frac{s}{m_e^2} - 1 \right), \quad (2)$$

which corresponds to  $\beta = 0.1235$  for  $\sqrt{s} = 500$  GeV.

Then the photon will be treated as if it had a measured value of  $\eta_{\text{meas}} = 0$ . By this procedure, the a priori knowledge of the photon's energy spectrum (in particular the fact that it is negligibly small in most cases) is used, and all energy and momentum constraints can be applied.

### 3 Performance tests

The method described above is applied to the process  $e^+e^- \rightarrow W^+W^- \rightarrow 4$  jets events. The fraction of successful fits, the width and the shift of the reconstructed  $W^\pm$  mass peak are used to compare the performance of the various kinematic fit variants.

#### 3.1 Data set

The analysis sample  $e^+e^- \rightarrow u\bar{d}\bar{d}u$  was generated using the matrix element generator WHIZARD [5], which takes into account all Feynman diagrams leading to a given final state, including interference terms.

The initial state radiation is also simulated by WHIZARD, the beamstrahlung spectrum is simulated with GUINEA-PIG [6]. For this calculation the nominal beam parameter set of the ILC was assumed.

A full simulation of the ILD detector [2] is performed by the GEANT based simulation program MOKKA [7]. In the event reconstruction, which is implemented as part of the software package MarlinReco [8], the tracks are matched to the calorimeter clusters by the Pandora particle flow algorithm [9] and the resulting reconstructed particles are forced into four jets by the Durham algorithm [10].

In order to investigate the influence of ISR and beamstrahlung on the performance of the kinematic fit, the results of all three fits are given for the complete event sample as well as for three subsamples with different amounts of ISR energy:  $E_{\text{ISR}} < 5$  GeV;  $5 \text{ GeV} \leq E_{\text{ISR}} \leq 30$  GeV and  $E_{\text{ISR}} > 30$  GeV.

#### 3.2 Evaluation method

In order to investigate the performance of the proposed method, kinematic fits are applied to the four jets in the events from the test sample, comparing the event hypotheses “4 jets” ( $4j$ ) and “4 jets + 1 photon” ( $4j + \gamma$ ). Both event hypotheses are fitted with five constraints (5C-fit): conservation of energy, conservation of the three momentum components and equal di-jet masses. In addition, the events are fitted also using only the three constraints (3C-fit) that are not affected by the presence of photon radiation, i.e. conservation of the transverse momentum components and the equal mass constraint.

Both values  $p_{z,\gamma} = 0$  and the missing  $p_z$  from the event  $p_{z,\gamma} = p_{z,\text{miss}}$  are considered as starting values for the photon momentum in the kinematic fit, and the result with the better fit performance is chosen.

The fits are compared in terms of the following three quantities: the fraction of fits with a fit probability  $> 0.001$ , the difference  $\Delta m_W = m_W - m_W^{\text{gen}}$  between the peak position of the reconstructed  $W^\pm$  mass spectrum and the input mass  $m_W^{\text{gen}} = 80.419$  GeV, and the Gaussian width of the peak. The latter two parameters have been determined from a fit to the mass spectrum which takes into account the natural width of the  $W^\pm$  and the small fraction of  $ZZ$  events in the sample [3]. Fig. 1 shows the the invariant di-jet masses before and after the kinematic fit for the complete sample, including ISR and beamstrahlung.

If large amounts of energy are missing, the fitted jet energies have to be larger than the measured ones to fulfill energy conservation. Consequently, di-jet masses are shifted to higher values and thus a larger  $\Delta m_W$  is obtained. Due to imperfections of the lineshape fit, a nonzero value of  $\Delta m_W$  is to be expected, for which a correction would be applied in a real analysis. However, if this mass shift depends on the amount of energy from ISR and beamstrahlung, it leads to a broadening of the signal and thus a loss of resolution; in addition, systematic uncertainties arise from the description of the ISR and in particular the beamstrahlung energy spectrum. Therefore, a mass shift that is independent of the amount of energy lost to ISR and beamstrahlung is desirable.

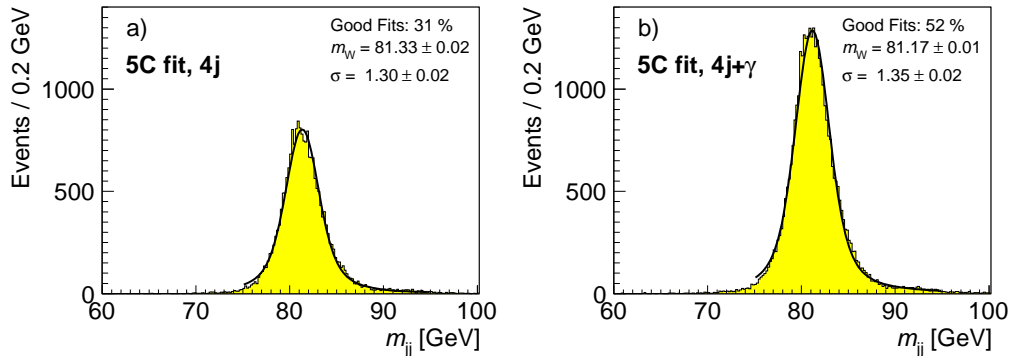


Figure 1: Invariant di-jet masses  $m_{jj}$  for the Monte Carlo sample described in the text: a) the di-jet masses  $m_{jj}$  for the 5C fit under a 4j hypothesis; b)  $m_{jj}$  for the 5C fit under a  $4j + \gamma$  hypothesis.

### 3.3 Results

Tab. 1 summarizes the results of our tests. It lists the fraction of good fits, the mass shift and the width of the Gaussian part of the peak for the complete sample, as well as the three subsamples with different amounts of missing energy due to ISR photons. The results are given for the average of the di-jet masses before a kinematic fit, using the 3C jet pairing, as well as the di-jet mass after applying a 3C fit or a 5C fit without or with an ISR photon. The results are reported for the case where the effect from beamstrahlung has been excluded, and for the realistic case where effects from ISR and beamstrahlung are fully taken into account.

Subsample (Fraction)	Constraints, Hypothesis	ISR only			Full Photon Spectrum		
		Good fits [%]	$\Delta m_W$ [GeV]	$\sigma_W$ [GeV]	Good fits [%]	$\Delta m_W$ [GeV]	$\sigma_W$ [GeV]
All events (100 %)	—	55 %	+0.78	2.05	55 %	+0.78	2.05
	3C, 4j	55 %	+0.82	2.06	55 %	+0.82	2.06
	5C, 4j	42 %	+0.67	1.21	31 %	+0.91	1.30
	5C, 4j + $\gamma$	54 %	+0.53	1.25	52 %	+0.75	1.35
$E_{\text{ISR}} < 5$ GeV (75 %)	—	56 %	+0.80	2.04	56 %	+0.80	2.04
	3C, 4j	56 %	+0.85	2.06	56 %	+0.85	2.06
	5C, 4j	53 %	+0.63	1.19	40 %	+0.86	1.27
	5C, 4j + $\gamma$	55 %	+0.49	1.24	54 %	+0.69	1.31
$5 \text{ GeV} \leq E_{\text{ISR}} \leq 30$ GeV (11 %)	—	54 %	+0.79	2.07	54 %	+0.79	2.07
	3C, 4j	54 %	+0.84	2.08	54 %	+0.84	2.08
	5C, 4j	15 %	+1.68	1.25	12 %	+2.19	1.29
	5C, 4j + $\gamma$	53 %	+0.71	1.27	50 %	+1.07	1.51
$E_{\text{ISR}} > 30$ GeV (13 %)	—	53 %	+0.59	1.99	53 %	+0.59	1.99
	3C, 4j	53 %	+0.66	1.99	53 %	+0.66	1.99
	5C, 4j	0 %	—	—	0 %	—	—
	5C, 4j + $\gamma$	47 %	+0.64	1.21	42 %	+0.91	1.38

Table 1: Results of kinematic fits under various conditions. “ISR only” refers to the case where the effect of beamstrahlung and beam energy spread is removed from the fit, while “Full Photon Spectrum” includes these effects. For each fit variation, the fraction of good fits with fit probability  $p > 0.001$ , the difference  $\Delta m_W$  between the fitted and generated W mass of  $m_W^{\text{gen}} = 80.419$  GeV, and the width of the Gaussian part of the peak is given. The rows refer to the results from averaging the measured di-jet masses without a fit for events where the 3C fit converges, the 3C fit with only transverse momentum and equal-mass constraint, the 5C fit under a four jet hypothesis with longitudinal momentum and energy constraints in addition, and the 5C fit with an additional ISR photon fit object. The subsamples are distinguished by the total energy  $E_{\text{ISR}}$  of ISR photons, excluding beamstrahlung.

### Results with ISR only

A comparison of the fit results demonstrates the gain in resolution achieved by kinematic fitting: The Gaussian  $\sigma$ , which corresponds to the di-jet mass resolution, is  $\sigma = 2.1$  GeV for the average of the two di-jet masses without a kinematic fit and improves to  $\sigma = 1.3$  GeV if a kinematic fit with five constraints is used. A fit with only three constraints does not improve the resolution compared to the simple averaging of the unfitted di-jet masses.

The fit with five constraints and no ISR photon cannot be applied to the subsample with  $E_{\text{ISR}} > 30$  GeV, because fit probabilities above the cut of  $p = 0.001$  are essentially never achieved due to the too large amounts of missing energy and momentum. Therefore this subsample, which contains 13 % of all events, cannot be used for an analysis. The 5C fit with an ISR photon, on the other hand, achieves almost the same performance for the two subsamples with  $E_{\text{ISR}} > 30$  GeV and  $E_{\text{ISR}} < 5$  GeV in terms of the fraction of good fits (47 % vs. 55 %) as well as in resolution ( $\sigma = 1.21$  GeV vs. 1.24 GeV) with only a small additional bias in the W mass ( $\Delta m_W = 0.64$  GeV vs. 0.49 GeV).

The sample with moderate ISR energy  $5 \text{ GeV} \leq E_{\text{ISR}} \leq 30 \text{ GeV}$ , which comprises 11 % of the events, demonstrates that the  $5C$  fit without the inclusion of an ISR photon tends to develop a mass bias. This is because the energy carried away by the photon is falsely attributed to the final state jets, which increases their energy and thus the invariant mass: The mass bias increases from  $\Delta m_W = +0.63 \text{ GeV}$  to  $+1.68 \text{ GeV}$ . At the same time, only 15 % of the events yield a good  $5C$  fit under the  $4j$  hypothesis. In contrast, the  $4j + \gamma$  hypothesis shows the same performance in terms of fraction of good fit, mass shift and resolution as for the sample with small missing energy.

The fact that for all fit hypotheses only about half of the events have reasonable fit probabilities  $p > 0.001$  can be mostly attributed to the equal-mass constraint: The resolution for the difference of the di-jet masses is approximately 4.1 GeV (twice the resolution for the di-jet mass average for the unfitted jets), which is of similar size as the broadening of 4.3 GeV due to the intrinsic  $W$  width. This indicates that in a real analysis the naïve equal-mass constraint has to be modified to take the natural  $W$  width into account. Other factors that reduce the fraction of successful fits are events from processes other than  $W/Z$  boson pair production and the fact that the jet error parametrization employed in this analysis does not include the effects of parton showering.

#### *Results with ISR and beamstrahlung*

The right-hand side of Tab. 1 shows the results for the case where the effect of both, ISR and beamstrahlung, is considered. Because the three subsamples are defined on the basis of the ISR energy only, the same amount of beamstrahlung is present in each of them. A comparison with the case where only the effect from ISR is considered, demonstrates that the photon momentum parametrization Eq. (1) derived from the ISR momentum spectrum also works quite well in the presence of beamstrahlung, at least at the level of beamstrahlung that is expected for the nominal ILC parameter set.

Since beamstrahlung in the Monte Carlo simulation used for this analysis is simulated solely through a variation of the energy of the incoming leptons, no transverse momentum is carried by the beamstrahlung. Therefore the results for the  $3C$  fit and the di-jet masses calculated without a kinematic fit do not change when beamstrahlung effects are considered.

The performance of the  $5C$  fit under the  $4j$  hypothesis is significantly reduced when beamstrahlung effects are considered due to the larger amount of missing energy. Overall, the fraction of good fits goes down from 42 % to 31 %. For the subsample with less than 5 GeV of ISR energy it is reduced from 53 % to 40 %. At the same time, the  $W^\pm$  mass shift increases by approximately 0.2 GeV for the whole sample. For the subsample with medium  $E_{\text{ISR}}$ , however, the mass shift increases from  $+1.68 \text{ GeV}$  to  $+2.19 \text{ GeV}$ .

On the other hand, with the  $4j + \gamma$  hypothesis, the  $5C$  fit performance is much less affected by beamstrahlung effects: The fraction of good fits stays almost constant, and the  $\sigma$  of the Gaussian width of the mass peak increases only moderately, from 1.25 GeV to 1.35 GeV for the complete sample. The mass shift increases by approximately 0.2 GeV for the full sample, which is similar to the  $4j$  hypothesis. However, for the subsample with  $5 \text{ GeV} \leq E_{\text{ISR}} \leq 30 \text{ GeV}$  the mass shift is significantly reduced from  $+2.19$  to  $+1.07 \text{ GeV}$  by the inclusion of the photon in the fit. The increase of the mass shift with respect to the ISR only case indicates that the  $4j + \gamma$  hypothesis cannot fully accommodate beamstrahlung effects, because typically both beam particles radiate off significant energy. This may necessitate the inclusion of a second photon in the fit.

As a final check, Fig. 2 shows the fitted longitudinal momentum  $p_{z,\gamma}$  of the photon versus the generated  $p_{z,\gamma}^{\text{gen}}$  of the most energetic ISR+beamstrahlung photon pair in the event, where the momenta of the ISR and beamstrahlung photons with either positive or negative  $p_z$  are added. It can be seen that the fitted photon momentum  $p_{z,\gamma}$  corresponds quite well to the true momentum, without any visible bias. In particular, the fact that the photon is treated as having a measured  $p_{z,\gamma} = 0$  does not lead to a large bias towards small values of  $p_{z,\gamma}$ . This is explained by the fact that the function  $p_{z,\gamma}(\eta)$  of Eq. (1) rises very rapidly.

The right side of Fig 2 shows the difference  $\Delta p_{z,\gamma} = \text{sign}(p_{z,\gamma}) \cdot (p_{z,\gamma} - p_{z,\gamma}^{\text{gen}})$ . The mean  $\langle \Delta p_{z,\gamma} \rangle = -0.32$  GeV is small, and negative, showing that the reconstructed  $|p_{z,\gamma}|$  is slightly smaller on average than the generated one, as expected, but that this bias is indeed quite small. The resolution for  $p_{z,\gamma}$  is found to be 3.25 GeV.

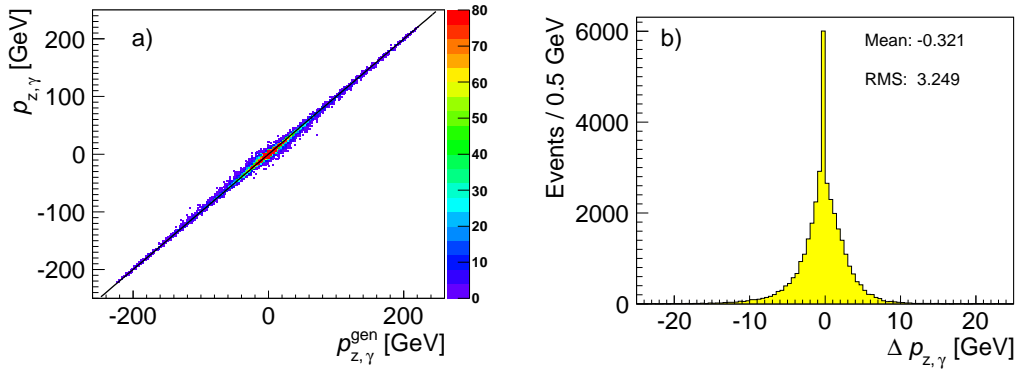


Figure 2: Fitted photon momentum  $p_{z,\gamma}$  plotted against the true momentum  $p_{z,\gamma}^{\text{gen}}$  of the most energetic ISR+beamstrahlung photon combination in the event (a), and the difference  $\Delta p_{z,\gamma} = \text{sign}(p_{z,\gamma}) \cdot (p_{z,\gamma} - p_{z,\gamma}^{\text{gen}})$  (b).

## 4 Summary and Conclusions

In this paper a method is proposed to take the effect of ISR into account in kinematic fits by introducing a photon that is treated as if its measured momentum were zero. The longitudinal momentum  $p_{z,\gamma}$  is expressed as a function  $p_{z,\gamma}(\eta)$  of the parameter  $\eta$  such that the true value of  $\eta$  follows a normal distribution with zero mean and unit standard deviation.

The performance of this method is evaluated using a sample of  $e^+e^- \rightarrow u\bar{d}d\bar{u}$  events, which is dominated by  $W^+W^-$  pair production, at  $\sqrt{s} = 500$  GeV. The sample includes the effects from ISR and beamstrahlung. It is fully simulated and reconstructed, using the simulation for the ILD detector at the ILC. A  $5C$  kinematic fit with energy and momentum conservation constraints and an equal-mass constraint is applied, and the results for the fit hypothesis with four jets and a photon are compared to three alternatives: a  $5C$  fit with a conventional four jet hypothesis, a  $3C$  fit where the energy and longitudinal momentum constraints are dropped, and the results obtained without a kinematic fit.

The  $5C$  fit with the new  $4j+\gamma$  hypothesis performs as well as a  $5C$  fit with a  $4j$  hypothesis in terms of resolution, while a  $3C$  is significantly worse and does not yield any improvement over a mass reconstruction without any kinematic fit.

For events with significant energy from ISR photons ( $5 \text{ GeV} \leq E_{\text{ISR}} \leq 30 \text{ GeV}$ ), the fraction of good fits with a fit probability  $p > 0.001$  drops from 40% to 12% for a  $5C$  fit without a photon, and goes to zero for  $E_{\text{ISR}} > 30 \text{ GeV}$ . In addition, as the missing energy is distributed to the jets by such a fit, a shift of the reconstructed di-jet masses towards larger values is observed.

Both problems are solved by the new  $4j + \gamma$  hypothesis: even for large values of  $E_{\text{ISR}} > 30 \text{ GeV}$ , the fraction of good fits and the di-jet mass resolution are similar to the values obtained at  $E_{\text{ISR}} < 5 \text{ GeV}$ , while the mass shift remains small.

In short, under the  $4j + \gamma$  hypothesis, a  $5C$  fit achieves the same resolution as with a conventional  $4j$  fit hypothesis, but independent of the amount of ISR energy, without developing a mass bias, and with a similar fraction of good fits as a  $3C$  fit.

Although the parametrization  $p_{z,\gamma}(\eta)$  was developed using the momentum spectrum of ISR photons, the method also performs well in the presence of beamstrahlung, at least at the moderate level expected for the nominal parameter set of the ILC.

In a future development the parametrization could be adapted to include beamstrahlung effects. This may be necessary in scenarios with enhanced beamstrahlung, such as the “low power” parameter set proposed for the ILC, or at CLIC. We expect that under such conditions the addition of a second photon in the fit would become necessary in order to take into account the energy loss suffered by both beam particles.

## Acknowledgements

We would like to thank the ILD simulation production team, in particular F. Gaede, S. Aplin, J. Engels and I. Marchesini, for the production of the samples of events used in this work, and T. Barklow for producing the generated input files.

We acknowledge the support of the DFG through the SFB (grant SFB 676/1-2006) and the Emmy-Noether program (grant LI-1560/1-1).

## References

- [1] M. A. Thomson, *Eur. Phys. J. C* **33** (2004) S689.
- [2] ILD Concept Group, “The International Large Detector — Letter of Intent,” DESY-2009-87 (2009).
- [3] M. Beckmann, B. List and J. List, “Treatment of Photon Radiation in Kinematic Fits at Future  $e^+e^-$  Colliders” arXiv:1006.0436 [hep-ex] (2010).
- [4] M. Beckmann, “Verbesserung der  $WW/ZZ$ -Unterscheidung am ILC durch Berücksichtigung von Photonabstrahlung in kinematischen Fits,” Diploma thesis, Leibniz University of Hannover (2009), DESY-THESIS-2010-014.
- [5] W. Kilian, T. Ohl and J. Reuter, “WHIZARD: Simulating multi-particle processes at LHC and ILC,” arXiv:0708.4233 [hep-ph] (2007).
- [6] D. Schulte, “Beam-beam simulations with GUINEA-PIG,” CERN-CLIC-NOTE-387 (1998).
- [7] “MOKKA: A detailed Geant4 simulation for the International Linear Collider detectors, version 06-07-p01,” <http://polzope.in2p3.fr:8081/MOKKA>.
- [8] O. Wendt, F. Gaede and T. Krämer, *Pramana* **69** (2007) 1109 [arXiv:physics/0702171].
- [9] M. A. Thomson, *AIP Conf. Proc.* **896** (2007) 215.
- [10] S. Bethke, Z. Kunszt, D. E. Soper and W. J. Stirling, *Nucl. Phys. B* **370** (1992) 310 [Erratum-ibid. B **523** (1998) 681].